Spring 5-2020

Dose response effect of Mycobacterium smegmatis-derived lipomannan in RAW 264.7 murine macrophages

Cassandra Robertson

Dose response effect of *Mycobacterium smegmatis*-derived lipoarabinomannan on RAW 264.7 murine macrophages

Cassandra Robertson

Senior Honors Project

Submitted in partial fulfillment of the graduation requirements of the Westover Honors College

Westover Honors College

University of Lynchburg

May 2020

_____

Dr. David Freier

_____

Professor Jeremy Craft

_____

Dr. Nancy Cowden

ABSTRACT

Tuberculosis is a debilitating respiratory disease caused by the bacterial species *Mycobacterium tuberculosis*, which acts by infecting the host's macrophages and evading their immune responses. The purpose of the study was to determine if RAW 264.7 murine macrophage activity could be facilitated and intensified by stimulation with LAM from *M. smegmatis*. Stimulation with bacterial LAM, and lipopolysaccharide (LPS) as a positive control, yields functional endpoints: nitric oxide (NO) production measured by nitrites (NO_2) in the culture supernatant and expression of proteins, such as tumor necrosis factor-α and inducible nitric oxide synthase (iNOS). RAW 264.7 cells were stimulated dose-responsively with LAM at concentrations of 1-1000 ng/mL. Use of 100 ng/mL LPS served as a positive control. Nitrite, an indirect product of the NO inflammatory response, was measured by the Greiss reaction and total protein was collected from the cells for western blotting to quantify iNOS. Preliminary results in experiment one showed that LAM NO production was minimally noticeable in the 1000 ng/mL dose and was still substantially lower than the LPS control when evaluated by the Greiss Assay. Experiments two and three were conducted with higher doses of Lam, 3000 ng/mL and 5000 ng/mL and showed an increased response. The nitrite concentration reached by both these LAM treatments still did not reach that of 100 ng/mL LPS. This result suggests that the pattern recognition difference between Toll-like receptor-2 (TLR-2) for LAM and Toll-like receptor-4 (TLR-4) for LPS has an impact on the output of NO.

INTRODUCTION

While the COVID-19 outbreak far overshadowed many significant anniversaries in the early part of 2020, the CDC annually recognizes March 24th as World TB Day. It marks the discovery of *Mycobacterium tuberculosis*, the bacterial species that causes the disease, by Dr. Robert Koch in 1882 (CDC 2016). This anniversary, though not a celebration, is a day for recognition of the infection that has been wreaking havoc on human populations for thousands of years. Tuberculosis (TB), historically referred to as scrofula, the White Plague, and consumption, is a respiratory disease and is transmittable from person to person via droplets from the sneezes or coughs of an actively infected individual (Tuberculosis 2018). The 2019 World Health Organization (WHO) TB report indicated that in 2018, there was a global estimate of 10 million people diagnosed with the illness and nearly 1.5 million deaths (WHO 2019). Caused by *Mycobacterium tuberculosis* (*Mtb*), this disease has evolved to be multi-drug resistant (MDR) and requires a grueling six-month course of antibiotics to cure. Health and research professionals often wonder how the ancient bacterial illness can still be so difficult to eradicate. The durability of the pathogen can be attributed to the presence of persister cells, a dormant variant of a normal cell that is slow growing and resistant to even high levels of antibiotics (Lewis 2010). These cells likely evolved as an adaptation from competing with the human immune system (Lougheed 2017). Since these cells make the infection particularly impervious, it is crucial to research and develop techniques that may improve the treatment process to more efficiently and effectively eliminate TB. This requires a thorough understanding of the pathways in which TB infects its host and how those mechanisms may be manipulated to weaken the bacteria.

In 2018 the WHO estimated that nearly one third of the world's population carries tuberculosis and that ten percent of those will acquire the infection, becoming a vector of the

disease. While these numbers seem underwhelming, an estimated 10.4 million new cases, 1.7 million being fatal, arose in 2016 (Tuberculosis 2018). The disease, caused by *Mtb* bacterial infection, often manifests as a respiratory infection but can also cause extrapulmonary disease to organ systems such as in lymph node TB, skeletal TB, and genitourinary TB (Fanning 1999). The disease is particularly virulent in those who become immunocompromised through age, another disease, or otherwise. In addition, many individuals with the infection have a latent form that may take years to unexpectedly activate. These factors lead to a bacterial contagion that aggressively eludes the human immune system and many modern treatment attempts.

Pathogens have individual characteristics that determine their virulence by impacting their hosts in unique ways. The distinguishing feature that heavily contributes to resilience is their defensive outer layer. The cell envelope of Gram-positive bacteria is composed of an inner membrane, phospholipid bilayer, surrounded by a thick layer of peptidoglycan that makes up the rigid cell wall (Salton and Kim 1996). In contrast, Gram-negative bacteria have a very thin layer of peptidoglycan separated from the inner membrane by periplasm and surrounded by another phospholipid bilayer, the outer membrane (Fig. 1). Gram-negative bacteria also contain lipopolysaccharide (LPS). Embedded in the outer membrane, the molecule activates the host immune system and acts as an endotoxin when the bacterial cell is attacked. Mycobacteria often resemble Gram-negative bacteria given the complexity of the cellular envelope; however, they possess a capsule instead of an outer membrane and some of their internal components are characteristic of only mycobacteria (Fig. 2). Lipomannan (LM) and lipoarabinomannan (LAM) are examples of essential compounds of the mycobacterial cell envelope, though their exact structural roles remain unclear (Fukuda et al. 2013).

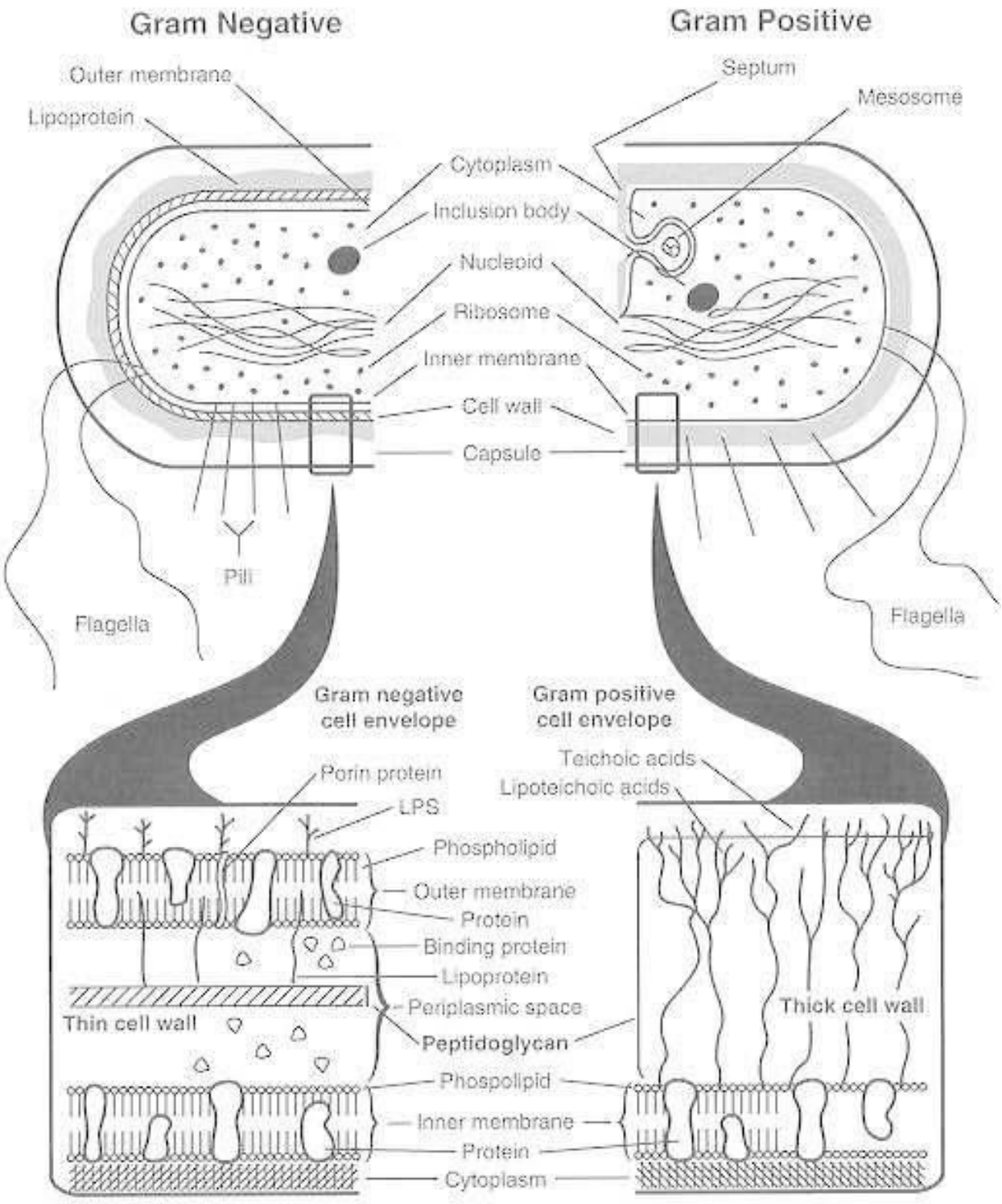

Figure 1: Comparison of the Gram-negative (left) and Gram-positive (right) cell envelopes. Gram-negative cells contain an inner membrane, a periplasmic space, a thin peptidoglycan layer, dense lipoproteins, and an outer membrane. Gram-positive bacteria contain an inner membrane and a thick wall of peptidoglycan (Salton and Kim 1996).

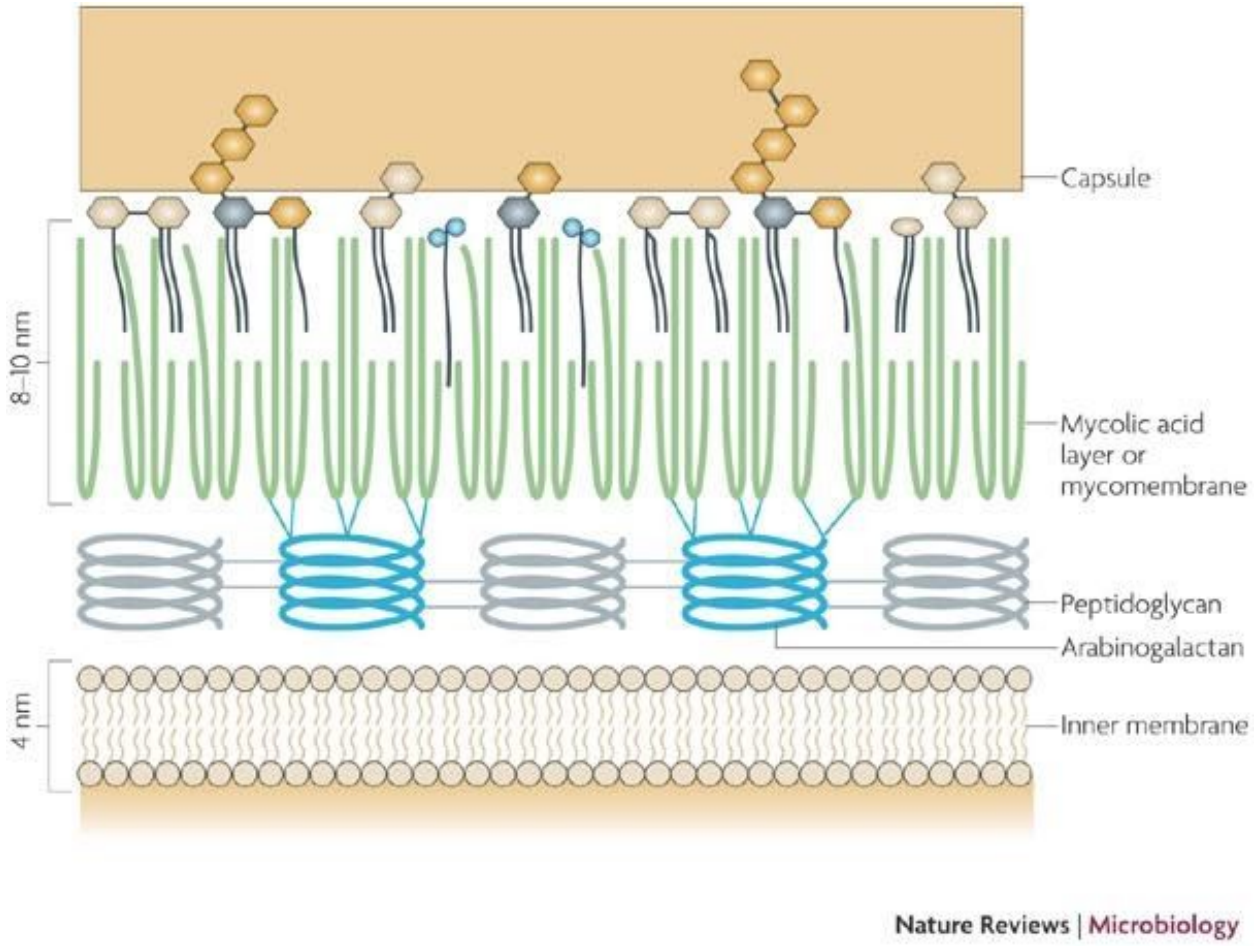

Figure 2: Diagram of a mycobacterial cell envelope. Layer from inside to out are inner membrane, peptidoglycan and arabinoglycan, mycolic acids and extractable lipids, and a capsule. LAM is anchored in the inner membrane and extends through the layers toward the capsule (Abdallah 2007).

Various proteins and polysaccharides contribute to the pathogenicity of mycobacterial species and especially serve as a physical barrier to host defensive processes.

When the human immune system comes into contact with foreign particles, there are a number of primary responders that identify whether or not the particle is a threat. When the innate immune system recognizes signature proteins in pathogens, such as LPS or LAM, the attack and elimination of the intruder begins. The macrophage is an important phagocyte, a cell type that engulfs foreign particles, and an initial responder in the innate immune system. Invaders are taken up as the cell membrane of the macrophage reaches around the particle, forming a pocket called a phagosome. Under normal operation, this phagosome containing harmful bacteria would be fused with a lysosome, releasing chemicals to destroy the bacteria (Slonczewski and Foster 2017). One of these chemicals is nitric oxide (NO), released by a protein called inducible nitric oxide synthase (iNOS). NO is responsible for killing many intracellular organisms, including some mycobacteria (Park et al. 2000). Though different species of microbes are vastly diverse in structure, there are a few common structural components such as LPS in Gram-negative bacteria, peptidoglycan in Gram-positive bacteria, and LAM in mycobacteria (Takeuchi and Akira 2001). These fundamental units activate the host's innate immune system and facilitate response to the pathogen.

Macrophages have many types of receptors through which mycobacterial particles bind, inducing the maturation of the phagosome (Daffé and Reyrat 2008). One example is the mannose receptor (MR). When TB comes in contact with the human immune system, mannose-capped LAM interacts with the MR on the surface of the macrophage, initiating the phagocytosis of *Mtb*. This specific activation of the MR from *Mtb* negatively impacts the development of the phagosome, reducing the capacity for phagolysosomal fusion (Daffé and Reyrat 2008). Toll-like

receptors (TLRs) also exist on the surface of phagocytic cells and upon reception of a recognized molecule, release pro-inflammatory cytokines. These substances, such as interleukin-1 (IL-1), interleukin-12 (IL-12), and tumor necrosis factor-α (TNF-α) mediate the inflammatory process and aid other immunological cells in their response to the invader (Dinarello 2000). LAM modulates the host immune system by preventing the release of pro-inflammatory cytokines IL-12 and TNF-α (Daffé and Reyrat 2008). The molecules aid leukocytes in adhering to endothelial cells before emigrating to tackle the infection (Dinarello 2000). Without these signaling molecules, other immune cells are not alerted to the presence of the disease and the immune response does not achieve maximum efficiency.

It is still largely unknown how *Mtb* evades the cytocidal properties of macrophages. In order to effectively target the disease, it is crucial to understand the pathway it takes to infect its host. While TLR-4 is responsible for recognition of LPS and the stimulation of iNOS to produce NO, there is evidence that LAM interacts with macrophages through TLR-2 (Takeuchi and Akira 2001). This difference could be responsible for the ability of *Mtb* to resist lysosomal degradation inside the phagocyte. One potential research avenue is to investigate the role of TLR-2 as *Mtb* evades the immune system. A second line of study is needed for better understanding of the stimulatory effects of mycobacterial LAM on macrophages. Previous research indicates that there are significant differences in the levels of response triggered by treatment of macrophages with LPS and LAM. In order to narrow-down the potential causes for this discrepancy, experiments that measure other inflammatory products must be explored.

Tuberculosis is a Bio-Safety Level 3 pathogen and it requires extreme caution and a negative airflow laboratory when cultured. Given the elevated risk, LAM from *Mycobacterium smegmatis* is utilized as a non-pathogenic model and substitute for LAM from *Mtb*.

Lipoarabinomannan from *M. smegmatis* is also accessible and practical for use in the lab. The LAM found in both *Mtb* and *M. smegmatis* is identical, except for capping variations that can occur in some strains of each species (Fig. 3) (Mishra et al. 2011). Without the capping molecules, the base structure for LAM of *Mtb* and *M. smegmatis* is identical.

An inevitable constraint encountered in all medical research is the ethics of testing and validating new technologies. In order to avoid breaching medical ethics, non-human animal and cellular models are often developed to take the place of what would otherwise need to be human-derived. A murine macrophage model has been developed as one standard for research on these monocytes. The RAW 264 cell line was established from tumors in mice with Abelson leukemia virus (Raschke et al. 1978). The strain of macrophages is immortal, meaning it can be maintained for an extended period of time by regularly transferring a sample of the cells to a new flask and replenishing nutrients. This enables the experimenters to perform multiple experiments on one original batch of cells. Specifically, the RAW 264.7 cell line has a well-established response to LPS and can be used to observe production of NO, iNOS, and TNF-α in response to bacterial infection. While human macrophages do not produce identical levels of NO, the murine macrophages serve as an effective model of human macrophage activity.

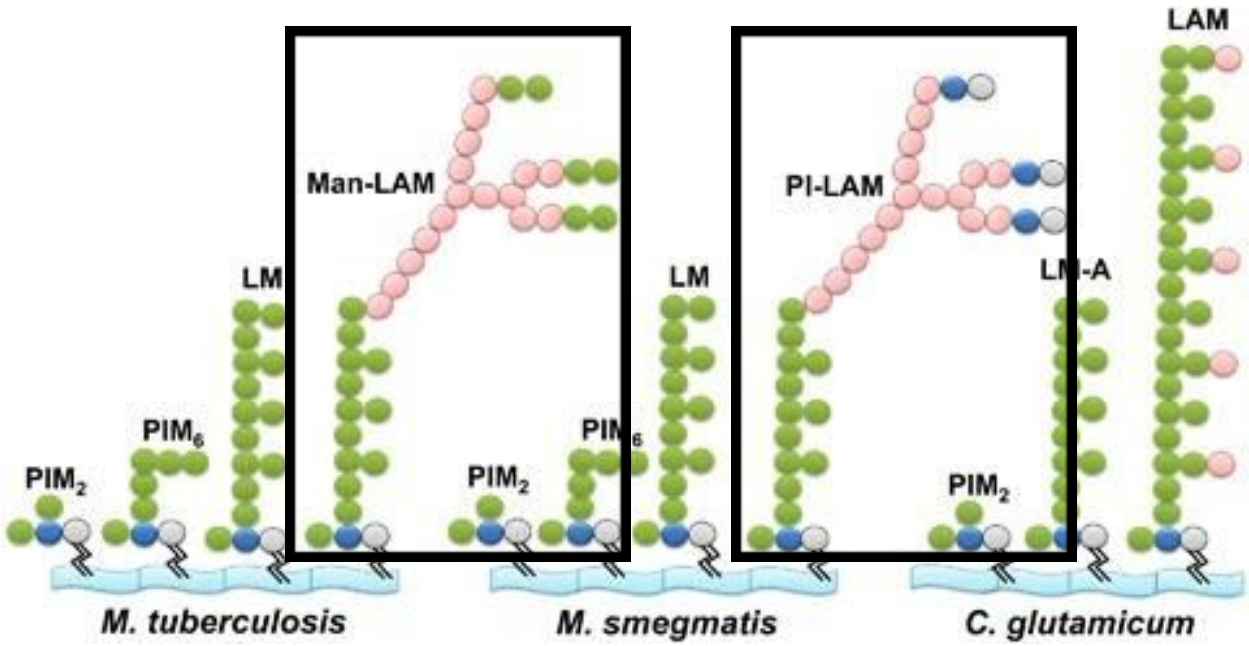

Figure 3: Structures of lipoarabinomannan and related glycoconjugates from the cell envelope of *M. tuberculosis*, *M. smegmatis*, and *C. glutamicum*. The black boxes indicate LAM variations in both *M. tuberculosis* (left) and *M. smegmatis* (right), identical except for their capping. The LAM found in *M. tuberculosis* is capped with mannose residues, making it Man-LAM. The LAM found in *M. smegmatis* is capped with phosphate (gray) and inositol (blue), making if PI-LAM (Adapted from Mishra et al. 2011).

The purpose of the study was to determine if RAW 264.7 murine macrophage activity could be facilitated and intensified by stimulation with LAM from *M. smegmatis*. The downstream effect is the production of inflammatory mediators, including NO and cytokines. The product observed was NO, quantified with the Greiss assay which measures the stable intermediate, nitrite. The expected results would indicate a dose-related response after stimulation with LAM from *M. smegmatis*. These levels were compared to the stimulation with LPS from *E. coli*, the positive control. If there is a significant difference in response levels from the two compounds, the signal transduction pathways connected to Toll-like receptors for both bacterial components will be explored in an attempt to identify the best method for measuring macrophage response to LAM.

MATERIALS AND METHODS

Cell Culture

The RAW 264.7 cells (ATCC; Manassas, VA) were cultured in DMEM complete, a solution containing DMEM with 4.5 g/L glucose and L-glutamine (Lonza/BioWhittaker; Walkersville, MD), 10% fetal bovine serum (Atlanta Biological, Lot#K13145; Flowery Branch, GA), $NaCO_3$ (Sigma-Aldrich; St. Louis, MO), and penicillin/streptomycin (Sigma-Aldrich; St. Louis, MO). Cells were grown in 25 cm^2 plastic flasks (CellTreat Scientific Products; Pepperell, MA) in an incubator (Shel Labs; Cornelius, OR) under the following conditions: 37°C, 5% CO_2, and 90% humidity. Passage of the cells occurred every 4 days by scraping and transferring to 5 mL of fresh media, maintaining a 1:20 cells to media ratio. The cells were stained with trypan blue and counted using a hemocytometer prior to each experiment in order to determine viability and cells per unit volume.

LAM Treatment

All experiments were performed between passes 5-20. In order to achieve a cell concentration of $0.8x10^6$ cells/mL, the appropriate volume of DMEM complete was added. A 24-well tissue culture plate (Costar Corning; Kennebunk, ME) was used and 500 µL of the cell suspension was aliquoted to each well, yielding $4.0x10^5$ cells/well. After 12-16 hours of incubation, the wells were washed twice with 500 µL DMEM. The LAM utilized in this experiment was derived from *Mycobacterium smegmatis* (InvivoGen; San Diego, CA) at a stock concentration of 0.33 µg/mL. The LPS used was from *Escherichia coli*, strain O55:B5 (Sigma-Aldrich; St. Louis, MO) and the stock concentration was 5 mg/mL. Treatment with LAM occurred in the following concentrations: 0 ng/mL, 1 ng/mL, 10 ng/mL, 100 ng/mL, 1000 ng/mL and 100 ng/mL LPS as a positive control. In order to maximize LAM response, an alternative

dose response experiment was executed at the following LAM concentrations: 0 ng/mL, 100 ng/mL, 1000 ng/mL, 3000 ng/mL, 5000 ng/mL, and 100 ng/mL LPS. All 24-well plates were incubated 24 hours following the addition of LAM or LPS for the induction of NO.

Greiss Assay

Sodium nitrite was used to create a standard curve of 1 μM to 125 μM nitrite along two duplicate rows in a 96-well plate. The treated 24-well plate was retrieved from the incubator and centrifuged for 2 minutes at 1000 rpm to remove any cell material from the supernatant. The layout of each 24-well plate was replicated by transferring 50 μL of supernatant from each treated well. The Greiss reagent was comprised of a 1:1 mixture of 1% sulfanilamide in 2.5% phosphoric acid and 0.1% napthylethylenediamene dihydrochloride in 2.5% phosphoric acid. Each well received 100 μL of the Greiss reagent. After about five minutes, a microplate reader (BioTek Epoch with Gen 5 software, BioTek Instruments Inc.; Winooski, VT) recorded the absorbance of each well at 550 nm and the results were exported to a spreadsheet. The standard curve from sodium nitrite was used to determine the nitrite concentrations of experimental samples. Each treatment was done in four replicate wells and these values were averaged.

Protein Isolation

A 200 μL sample was removed from each sample well of the 24-well plate to be frozen (at -80°C) for future cytokine analysis. Then total protein was collected from each well to be used for western blotting. The RIPA mixture was made using 3 mL RIPA buffer (with triton X-100; Boston Bioproducts; Worcester, MA), 15 μL bovine lung Aprotinin (Sigma-Aldrich; St. Louis, Missouri), 15 μL Sigma P8340 protease inhibitor cocktail (Sigma-Aldrich; St. Louis, Missouri), and 6 μL 0.5M EDTA (Sigma-Aldrich; St. Louis, Missouri). Each well was washed twice with 500 μL PBS (calcium/magnesium-free phosphate buffered saline; Sigma-Aldrich; St.

Louis, Missouri) and received 100 µL of the RIPA mixture. After five minutes, a pipette tip was used to scrape and triturate each well. All four wells containing the same treatment concentration were consolidated into an individual microcentrifuge tube (USA Scientific; Orlando, FL), all of which were stored in the -80°C freezer.

Bradford Assay

A protein standard curve was created using five stepwise dilutions from 2mg/mL Bovine Serum Albumin (BSA; Sigma-Aldrich; St. Louis, Missouri). The dilutions of 5, 10, 20, 40, and 80 µg BSA were placed in a 96-well plate in 200 µL aliquots across the top row. In the second row, 1 µL samples from the isolated RAW 264.7 proteins were inserted into 159 µL diH_2O. Each well containing sample received 40 µL of Bradford reagent (BioRad Laboratories; Hercules, CA). The liquids were triturated to ensure thorough color dispersion. Trituration was performed to ensure the Coomassie Blue interacted and bonded with the proteins. The plate was inserted into the BioTek microplate reader and absorbance was measured at 595 nm. The standard curve from BSA was used to determine the protein concentrations of experimental samples.

Statistical Analysis

Using SSPS (Ver. 25.0; IBM Corp.; Armack, NY, USA), the results were analyzed in a one-way ANOVA test. This was used to determine significant differences between LAM dose responses. A post-hoc analysis using a two-sided Dunnett's t-test was performed to identify significance from the negative control, 0 ng/mL LAM. Significance occurred when $P \leq 0.05$.

RESULTS

The RAW 264.7 macrophages were treated with LAM and LPS over a 24-hour window and the nitrite concentration was measured with a Greiss assay. In the initial experiment, the 1.0 ng/mL, 10 ng/mL, and 100 ng/mL LAM conditions did not exceed 5 μM nitrite and were not significantly different than the concentration of nitrite in the negative control (Fig. 4). The 1000 ng/mL LAM response averaged 6.1 μM nitrite. The 100 ng/mL LPS positive control reached a nitrite concentration of 52.1 μM (Fig. 4). Significance occurred only in the LPS positive control and not in any LAM treatments (Appendix A). Given the low levels yielded by LAM treatment in experiment 1, an additional protocol was developed to include doses of higher concentrations.

In experiment 2, the 1.0 ng/mL and 10 ng/mL treatments were replaced with 3000 ng/mL and 5000 ng/mL. The macrophages universally achieved increased output of NO as the nitrite concentration reached 12.9 μM in the 1000 ng/mL LAM dose. The 3000 ng/mL and 5000 ng/mL LAM treatments produced responses of 21.6 μM and 38.1 μM nitrite, respectively (Fig. 5). In this experiment, the positive control produced 72.7 μM nitrite in response to 100 ng/mL LPS. Only the 100 ng/mL LAM treatment was not significant when compared to the negative control (Appendix B). Two repetitions with the treatments 100-5000 ng/mL LAM showed similar responses. However, all conditions in experiment 3 yielded lower nitrite concentrations (Fig. 6). The results of the 100 ng/mL and 1000 ng/mL LAM doses were not statistically significant (Appendix C). The 3000 ng/mL and 5000 ng/mL LAM treatments, as well as 100 ng/mL LPS, showed significance from the negative control (Appendix C).

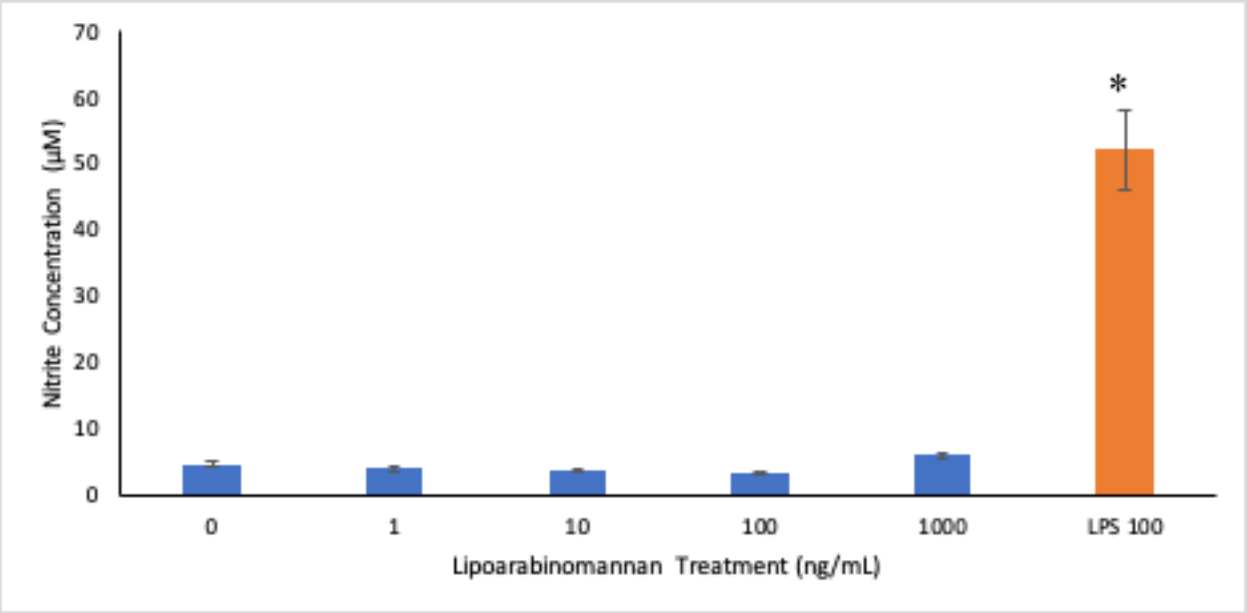

Figure 4: Preliminary stimulation of RAW 264.7 murine macrophages with LAM derived from *M. smegmatis.* Initial dose response experiment measured by Greiss reaction used treatments of 1.0-1000 ng/mL LAM (blue bars). Negative and positive controls were 0 ng/mL LAM and 100 ng/mL LPS (orange bar), respectively. Absorbance recorded at 550 nm. The bars represent the ± standard deviation among the four treatment wells. *P ≤ 0.05 in one-way ANOVA with Dunnett's post-hoc t-test analysis.

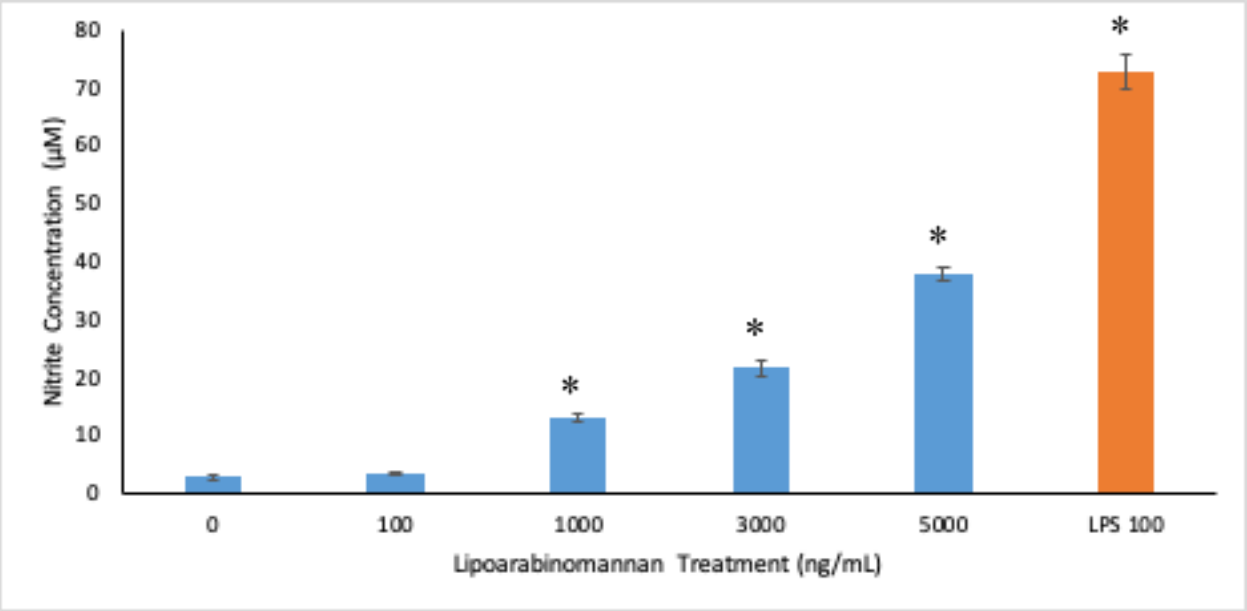

Figure 5: Experiment 2 of RAW 264.7 murine macrophages stimulated with LAM derived from *M. smegmatis.* Dose response experiment measured by Greiss reaction used treatments of 100-5000 ng/mL LAM (blue bars). Negative and positive controls were 0 ng/mL LAM and 100 ng/mL LPS (orange bar), respectively. Absorbance recorded at 550 nm. The bars represent the ± standard deviation among the four treatment wells. *P ≤ 0.05 in one-way ANOVA with Dunnett's post-hoc t-test analysis.

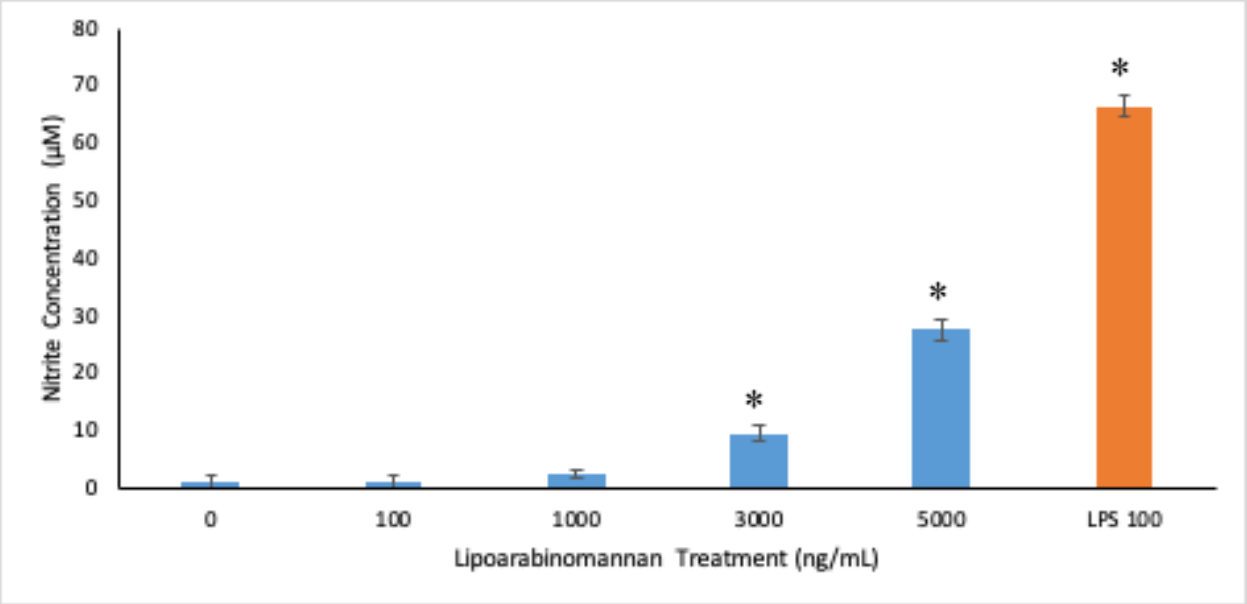

Figure 6: Experiment 3 of RAW 264.7 murine macrophages stimulated with LAM derived from *M. smegmatis.* Dose response experiment measured by Greiss reaction used treatments of 100-5000 ng/mL LAM (blue bars). Negative and positive controls were 0 ng/mL LAM and 100 ng/mL LPS (orange bar), respectively. Absorbance recorded at 550 nm. The bars represent the ± standard deviation among the four treatment wells. *P ≤ 0.05 in one-way ANOVA with Dunnett's post-hoc t-test analysis.

DISCUSSION

The purpose of this study was to determine if RAW 264.7 murine macrophages would show dose-responsive activity when treated with LAM derived from *M. smegmatis*. It was predicted that the interaction of LAM with the TLR-2 signaling pathway would increase NO output, and ultimately nitrite concentration, when dosed with increasing concentrations of LAM. The positive control of LPS from *E. coli* was used to determine if the magnitude of LAM response was comparable to a common standard. The results indicate that LAM can stimulate a dose-dependent, inflammatory response in murine macrophages.

In a previous report, Zaman (2019) conducted two congruent trials similar to those in this study. Her preliminary experiment, compatible with experiment 1, showed significance at the 100 ng/mL and 1000 ng/mL LAM doses, yielding approximately 8 μM and 55 μM nitrite respectively (Zaman 2019). There was also significance in the 100 ng/mL LPS control which produced approximately 104 μM (Zaman 2019). The second experiment performed by Zaman (2019) was identical to experiment 2 in this investigation, with the addition of 10 ng/mL and 2000 ng/mL LAM treatments. A dose-response effect of LAM was observed between 1000 and 5000 ng/mL and was determined to be significantly different from untreated controls (Zaman 2019). Her data indicates a response of approximately 65 μM nitrite in the 5000 ng/mL LAM treatment, while the data from experiments 2 and 3 here show only 38.1 μM and 27.5 μM nitrite respectively. While similar trends exist between the two studies, the results of Zaman (2019) far exceeded the output of NO found in the data of this report. A potential explanation for these discrepancies could be the less than ideal growth conditions the RAW cells experienced due to damaged incubators. Despite the fact that this study yielded lower responses, the dose-response trends are analogous to those found by Zaman (2019) and show that LAM can induce dose-related NO production in RAW 264.7 murine macrophages. The results are in accordance

with other sources that indicate RAW cell stimulation with LAM can produce a NO response (Park et al. 2000).

After analyzing the data of all three experiments, adjacent with those of Zaman (2019), it is evident that the RAW 264.7 murine macrophages are not as sensitive to LAM as they are LPS. There are several possibilities to explain this phenomenon, some of which refer to the different receptors through which each compound interacts with the macrophage. Since TLRs each bind with unique ligands, the difference could be a result of LPS interacting with TLR-4 and LAM with TLR-2. While it is difficult to find research on specific affinities of TLRs, it is likely that they fluctuate among the TLRs, potentially causing the response difference of LAM and LPS. The quantity of each TLR on the surface of the macrophage could also play a role in the level of response. If the presence of TLR-4 is far greater than that of TLR-2, it would be expected to see a diminished activation of the macrophages when treated with LAM. Additional research should be conducted in order to examine the effect of supplementary molecules on the NO production of macrophages.

Limitations encountered when conducting this research included both local and global disruptions. Due to the halted and incomplete renovation of laboratory facilities, research that should have commenced in August of 2019, did not begin until January of 2020. At the end of February, the primary cell culture incubator suffered a thermostat malfunction, causing temperature regulation to fail. An alternative incubator was set up for use and the cells were transferred. This incubator, however, did not maintain proper humidity because of inconsistent CO_2 regulation. Finally, March brought with it the news that classes would resume online after Spring break as a result of the COVID-19 outbreak. This prevented further experimentation which would have augmented the presented data. These protocols would have included using

ELISA for quantification of TNF-α and western blot analysis of iNOS. The original intentions of this study were to compare the relative NO output to the presence of both TNF-α and iNOS. If the research is to be continued, one could compare the TLR-4 and TLR-2 pathways, exploring the impact they have on the output of NO and pro-inflammatory cytokines.

The results of the present study contribute on a small scale to the overall knowledge of interactions between LAM and macrophages. By knowing the extent at which LAM activates macrophage production of NO, scientists can begin to grasp the downstream effects of *Mtb* invasion. Research shows that pathogenic mycobacterial LAM acts as an intercalating agent that stunts phagosomal maturation (Guenin-Macé et al. 2009). Additionally, LAM from *Mtb* inhibits the production of pro-inflammatory cytokines, such as IL-12, preventing the development of other critical immune cells (Guenin-Macé et al. 2009). A thorough understanding of the molecular pathways of infection is vital for the improvement of TB treatments and medication. Given the continued severity and prevalence of the disease, the diagnosis and treatment of the disease has never been more crucial. Research in this field must continue in an attempt to more effectively target the processes which make the infection so virulent.

REFERENCES

Abdallah AM. 2007. Type VII secretion – mycobacteria show the way. Nature Reviews Microbiology. 5(11): 883-891.

Center for Disease Control. 2016. World TB Day [Internet]. Available from: https://www.cdc.gov/tb/worldtbday/history.htm

Daffé M and Reyrat J-M. 2008. *The mycobacterial cell envelope.* Washington (DC): ASM Press.

Dinarello CA. 2000. Proinflammatory cytokines. Chest. 118(2): 503-508.

Fanning A. 1999. Tuberculosis: 6. Extrapulmonary disease. Canadian Medical Association Journal. 160: 1597-1603.

Fukuda T, Matsumura T, Ato M, Hamasaki M, Nishiuchi Y, Murakami Y, Maeda Y, Yoshimori T, Matsumoto S, Kobayashi K, Kinoshita T, Morita YS. 2013. Critical roles for lipomannan and lipoarabinomannan in cell wall integrity of mycobacteria and pathogenesis of tuberculosis. mBio. 4(1): e00472-12.

Guenin-Macé L, Siméone R, Demangel C. 2009. Lipids of pathogenic mycobacteria: Contributions to virulence and host immune suppression. Transboundary and Emerging Diseases 56(6-7):255-68.

Lewis K. 2010. Persister cells. Annual Review of Microbiology. 64(1): 357-372.

Lougheed K. 2017. Killing the unkillable [Internet]. Bloomsbury Publishing Plc; [cited 2020 Mar 23]. Available from: http://www.naturalhistorymag.com/features/073313/killing-the-unkillable

Mishra AK, Essen NN, Appelmelk BJ, Besra GS. 2011. Lipoarabinomannan and related glycoconjugates: Structure, biogenesis and role in mycobacterium tuberculosis physiology and host-pathogen interaction. FEMS Microbiology Reviews. 35(6):1126-57.

Park E, Levis WR, Quinn MR, Park SY, Schuller-Levis GB. 2000. Regulation of nitric oxide induced by mycobacterial lipoarabinomannan in murine macrophages: effects of interferon-β and taurine-chloramine. International Journal of Leprosy. 68(4): 444-451.

Raschke WC, Baird S, Ralph P, Nakoinz I. 1978. Functional macrophage cell lines transformed by Abelson Leukemia Virus. Cell. 15(1): 261-267.

Salton MRJ and Kim KS. Structure. 1996. In: Baron S. *Medical Microbiology*. Fourth edition. Galveston, TX: University of Texas Medical Branch at Galveston.

Slonczewski JL and Foster JW. 2017. Human Microbiota and Innate Immunity. In: Betsy Twitchell. *Microbiology: an evolving science.* Fourth edition. New York, NY: W. W. Norton & Company, Inc. p. 920-921.

Takeuchi O and Akira S. 2001. Toll-like receptors; their physiological role and signal transduction system. International Immunopharmacology. 1(4):625-35.

Tuberculosis [Internet]. c2018. World Health Organization. [updated 2018 Feb 26; cited 2019 Dec 13]. Available from: https://www.who.int/immunization/diseases/tuberculosis/en/

World Health Organization. 2019. Global tuberculosis report [Internet]. Available from: https://www.who.int/tb/publications/global_report/en/

Zaman A. (2019). Lipoarabinomannan from *Mycobacterium smegmatis* stimulates an inflammatory response in RAW 264.7 murine macrophages (Unpublished undergraduate thesis). University of Lynchburg, Lynchburg, Virginia, USA.

APPENDIX A

Statistical analysis of experiment 1 and the data represented in Figure 4. One-way ANOVA with Dunnett's host-hoc t-test analysis. Significance indicated when $P \leq 0.05$.

Oneway

ANOVA

LAM Data

	Sum of Squares	df	Mean Square	F	Sig.
Between Groups	7334.461	5	1466.892	252.152	.000
Within Groups	104.715	18	5.817		
Total	7439.176	23			

Post Hoc Tests

Multiple Comparisons

Dependent Variable: LAM Data

Dunnett t (2-sided)[a]

		Mean			95% Confidence Interval	
(I) V1	(J) V1	Difference (I-J)	Std. Error	Sig.	Lower Bound	Upper Bound
1	6	-.54750	1.70551	.997	-5.2571	4.1621
2	6	-.77000	1.70551	.988	-5.4796	3.9396
3	6	-1.22750	1.70551	.921	-5.9371	3.4821
4	6	1.45500	1.70551	.860	-3.2546	6.1646
5	6	46.63500*	1.70551	.000	41.9254	51.3446

*. The mean difference is significant at the 0.05 level.

a. Dunnett t-tests treat one group as a control, and compare all other groups against it.

APPENDIX B

Statistical analysis of experiment 2 and the data represented in Figure 5. One-way ANOVA with Dunnett's host-hoc t-test analysis. Significance indicated when $P \leq 0.05$.

Oneway

ANOVA

LAM data

	Sum of Squares	df	Mean Square	F	Sig.
Between Groups	14234.493	5	2846.899	1362.747	.000
Within Groups	37.604	18	2.089		
Total	14272.097	23			

Post Hoc Tests

Multiple Comparisons

Dependent Variable: LAM data

Dunnett t (2-sided)[a]

		Mean			95% Confidence Interval	
(I) V1	(J) V1	Difference (I-J)	Std. Error	Sig.	Lower Bound	Upper Bound
1	6	.41000	1.02203	.993	-2.4122	3.2322
2	6	10.00000*	1.02203	.000	7.1778	12.8222
3	6	18.67500*	1.02203	.000	15.8528	21.4972
4	6	35.20250*	1.02203	.000	32.3803	38.0247
5	6	69.74750*	1.02203	.000	66.9253	72.5697

*. The mean difference is significant at the 0.05 level.

a. Dunnett t-tests treat one group as a control, and compare all other groups against it.

APPENDIX C

Statistical analysis of experiment 3 and the data represented in Figure 6. One-way ANOVA with Dunnett's host-hoc t-test analysis. Significance indicated when $P \leq 0.05$.

Oneway

ANOVA

LAM/LPS µM Concentration

	Sum of Squares	df	Mean Square	F	Sig.
Between Groups	13283.182	5	2656.636	1422.596	.000
Within Groups	33.614	18	1.867		
Total	13316.796	23			

Post Hoc Tests

Multiple Comparisons

Dependent Variable: LAM/LPS µM Concentration

Dunnett t (2-sided)[a]

		Mean			95% Confidence Interval	
(I) V1	(J) V1	Difference (I-J)	Std. Error	Sig.	Lower Bound	Upper Bound
1	6	.20000	.96630	1.000	-2.4683	2.8683
2	6	1.47250	.96630	.433	-1.1958	4.1408
3	6	8.45500*	.96630	.000	5.7867	11.1233
4	6	26.47250*	.96630	.000	23.8042	29.1408
5	6	65.43250*	.96630	.000	62.7642	68.1008

*. The mean difference is significant at the 0.05 level.

a. Dunnett t-tests treat one group as a control, and compare all other groups against it.